

ORIGINAL RESEARCH

Rieske FeS overexpression in tobacco provides increased abundance and activity of cytochrome *b₆f*

Eiri Heyno¹  | Maria Ermakova^{1,2}  | Patricia E. Lopez-Calcagno^{3,4}  |
 Russell Woodford¹  | Kenny L. Brown³  | Jack S. A. Matthews³  |
 Barry Osmond¹  | Christine A. Raines³  | Susanne von Caemmerer¹ 

¹Centre of Excellence for Translational Photosynthesis, Division of Plant Science, Research School of Biology, The Australian National University, Acton, Australian Capital Territory, Australia

²School of Biological Sciences, Monash University, Melbourne, Victoria, Australia

³School of Biological Sciences, University of Essex, Colchester, UK

⁴School of Natural and Environmental Sciences, Newcastle University, Newcastle, UK

Correspondence

Eiri Heyno and Maria Ermakova, Centre of Excellence for Translational Photosynthesis, Division of Plant Science, Research School of Biology, The Australian National University, Acton, Australian Capital Territory 2601, Australia.

Email: eiri.heyno@anu.edu.au and maria.ermakova@anu.edu.au

Funding information

Realizing Increased Photosynthetic Efficiency, Bill and Melinda Gates

Edited by A. Krieger-Liszky

Abstract

Photosynthesis is fundamental for plant growth and yield. The cytochrome *b₆f* complex catalyses a rate-limiting step in thylakoid electron transport and therefore represents an important point of regulation of photosynthesis. Here we show that overexpression of a single core subunit of cytochrome *b₆f*, the Rieske FeS protein, led to up to a 40% increase in the abundance of the complex in *Nicotiana tabacum* (tobacco) and was accompanied by an enhanced in vitro cytochrome *f* activity, indicating a full functionality of the complex. Analysis of transgenic plants overexpressing Rieske FeS by the light-induced fluorescence transients technique revealed a more oxidised primary quinone acceptor of photosystem II (*Q_A*) and plastoquinone pool and faster electron transport from the plastoquinone pool to photosystem I upon changes in irradiance, compared to control plants. A faster establishment of *q_E*, the energy-dependent component of non-photochemical quenching, in transgenic plants suggests a more rapid buildup of the transmembrane proton gradient, also supporting the increased in vivo cytochrome *b₆f* activity. However, there was no consistent increase in steady-state rates of electron transport or CO₂ assimilation in plants overexpressing Rieske FeS grown in either laboratory conditions or field trials, suggesting that the in vivo activity of the complex was only transiently increased upon changes in irradiance. Our results show that overexpression of Rieske FeS in tobacco enhances the abundance of functional cytochrome *b₆f* and may have the potential to increase plant productivity if combined with other traits.

1 | INTRODUCTION

Global crop production needs to double by 2050 to meet the needs of increasing human and cattle populations and biofuel consumption (Ray et al., 2013). The green revolution has brought many parameters of crop yield potential close to the theoretical maximum, the most significant ones being the efficiency of biomass partitioning into harvested products and

the efficiency of solar radiation capture. Modelling studies suggest that there is still significant potential to increase the efficiency of photosynthesis, the major contributor to plant growth (Bailey-Serres et al., 2019; Evans, 2013; Long et al., 2006; Ort et al., 2015; Parry et al., 2013). This has led to research efforts focusing on improving various photosynthetic components in an attempt to improve plant productivity (Ermakova et al., 2021; Kromdijk et al., 2016; López-Calcagno et al., 2019).

Photosynthetic electron transport is responsible for providing ATP and NADPH for photosynthetic carbon reduction, and it is suggested to

Eiri Heyno, Maria Ermakova, and Patricia E. Lopez-Calcagno contributed equally to this work.

This is an open access article under the terms of the [Creative Commons Attribution](https://creativecommons.org/licenses/by/4.0/) License, which permits use, distribution and reproduction in any medium, provided the original work is properly cited.

© 2022 The Authors. *Physiologia Plantarum* published by John Wiley & Sons Ltd on behalf of Scandinavian Plant Physiology Society.

limit CO₂ assimilation rates at ambient and high CO₂ partial pressures (von Caemmerer & Farquhar, 1981; Yamori et al., 2010). Light energy, captured by light-harvesting pigments, drives electron transport through the thylakoid membranes of chloroplasts. The cytochrome *b₆f* complex (Cytb₆f) plays a central role in the electron transport chain as it functions as an electron hub between photosystem II (PSII) and photosystem I (PSI), and its proton pumping activity is the main contributor to the acidification of the thylakoid lumen. Cytb₆f also has a unique role in electron transport because it is involved in both linear electron transport, carried out by both photosystems to produce ATP and NADPH, and cyclic electron transport around PSI for the generation of ATP alone. Transmembrane proton gradient (Δ pH) established across the thylakoid membrane during the electron transport is the main component of the proton motive force (*pmf*) used by the ATP synthase complex to produce ATP. In addition, Δ pH exerts control over the rate of electron transport by feedback regulation of PSII activity via non-photochemical quenching (NPQ) that dissipates a part of light energy absorbed in the PSII antennae as heat before it reaches the reaction centres (Ruban, 2016). In plants, the major quickly reversible component of NPQ (*q_E*) is mediated by the PsbS protein acting as a luminal pH sensor and by violaxanthin de-epoxidase converting violaxanthin to zeaxanthin in the PSII antennae (Johnson et al., 2009).

Cytb₆f catalyses the slowest reaction in the electron transport chain (Tikhonov, 2014). Moreover, acidification of the lumen further slows down the Cytb₆f activity, a phenomenon known as photosynthetic control (Colombo et al., 2016). Previous works on transgenic tobacco plants with reduced abundance of the Rieske FeS protein (hereafter Rieske), one of the core subunits of Cytb₆f encoded by the nuclear *petC* gene, demonstrated a strong correlation between the amount of the complex in the thylakoid membrane and leaf electron transport rate (Price et al., 1995; Price et al., 1998; Ruuska et al., 2000; Yamori et al., 2011). Similar results were observed in rice, where plants with reduced Cytb₆f content showed decreased grain yield (Yamori et al., 2016). Overexpression of Rieske in the model C₃ and C₄ species, *Arabidopsis thaliana* and *Setaria viridis*, led to increases in electron transport and CO₂ assimilation rates, suggesting that it is a promising route to boost crop productivity (Ermakova et al., 2019; Simkin et al., 2017).

Here we explored the effect of Rieske overexpression (Rieske-OE) in the model crop plant *Nicotiana tabacum* (tobacco). We show that increasing Rieske content provides up to a 20% increase in functional Cytb₆f, as confirmed by the cytochrome *f* (CytF) activity, but without marked changes in steady-state electron transport or CO₂ assimilation rates. Our detailed functional analysis of electron transport using light-induced fluorescence transients (LIFT) technique and spectroscopic measurements confirmed higher Cytb₆f activity in plants with increased Rieske content. Our results indicate that, at tested CO₂ and irradiance regimes, Cytb₆f activity is not the only factor limiting electron transport rate in tobacco.

2 | MATERIALS AND METHODS

2.1 | Generation of construct and transgenic plants

The construct for Rieske-OE (Figure S1) was created using the Golden Gate cloning system (Engler et al., 2014). The coding sequence of the

A. thaliana *PetC* gene (AT4G03280) was assembled with the *A. thaliana* *RbcS2B* (AT5G38420) promoter and the *A. thaliana* *HEAT SHOCK PROTEIN 18.2* terminator (AT5G59720). The construct contained two selection markers: the bialaphos resistance gene (*bar*) under the control of the nopaline synthase promoter (*pNOS*) and the hygromycin phosphotransferase gene (*HPT*) under the control of the cauliflower mosaic virus 35 *S* promoter. The resulting plasmid was introduced into *N. tabacum* cv. Petit Havana using *Agrobacterium tumefaciens* strain LBA4404 via leaf-disc transformation (Horsch et al., 1985). The shoots were regenerated on Murashige and Skoog medium containing 20 mg L⁻¹ hygromycin and 400 mg L⁻¹ cefotaxime. Resistant primary transformants (T₀ generation) with established roots were transferred to soil and allowed to self-fertilise. T₀ plants were analysed for the *HPT* copy number (iDNA genetics). Homozygous and azygous plants were selected in the T₁ generation. All experiments were conducted on T₂ plants. WT plants were used as control for most experiments, except for the field trials where a combination of WT and azygous plants were used.

2.2 | RNA isolation and qPCR

Total RNA was extracted from tobacco leaf discs sampled from T₁ plants and quickly frozen in liquid nitrogen using the NucleoSpin[®] RNA Plant Kit (Macherey-Nagel). cDNA was synthesised using 1 μ g of total RNA according to the protocol in the RevertAid Reverse Transcriptase kit (Fermentas). Transcript abundance of *AtPetC* and *NtActin* in cDNA samples was estimated using primers AACGCC-CAAGGAAGAGTCGT and ACCACCATGGAGCATCACCA for *AtPetC* and CCTGAGGTCCTTTTCCAACCA and GGATTCCGGCAGCTTC-CATT for *NtActin* (Schmidt & Delaney, 2010). For qPCR, the SensiFAST SYBR No-ROX Kit was used according to the manufacturer's recommendations (Bioline Reagents Ltd.).

2.3 | Plant growth conditions

For physiological analyses (Figures 4–7), plants were grown from seeds in 2.8–4.5 L pots filled with potting mix and topped with seed raising mix, both supplemented with 7 g L⁻¹ of slow-release fertiliser (Osmocote). Plants were grown in controlled environment rooms at ambient CO₂, 12/12 h day/night photoperiod, 24/20°C day/night and 55% relative humidity with light at 400 μ mol m⁻² s⁻¹ supplied by 1000 W red sunrise 3200 K lamps (Sunmaster Grow-lamps). For the thylakoid isolation (Figures 2 and 3), plants were grown in cabinets in the same conditions and the illumination was supplied by a mixture of fluorescent tubes (Master TL5 HO 54 W/840, Philips Lighting) and halogen incandescent globes (42 W 2800 K warm white clear glass 630 lumens, CLA). A subset of lines (R17, R20, R26) for the thylakoid isolation was grown in a commercial potting mix supplemented with 2 g L⁻¹ of Osmocote; the CytF activity measured from the WT thylakoids grown in different potting mixes did not differ (Figure S4). All experiments were

performed on the first fully expanded leaves (third or fourth from the top) of 4–5 week-old plants.

2.4 | Gas exchange

The net rates of CO₂ assimilation were measured using a portable gas exchange system LI-6800 (LI-COR Biosciences) equipped with the Fluorometer head 6800-01A (LI-COR Biosciences) under red-blue (90/10%) actinic light. Before the measurements, plants were adapted for 30 min to 1500 μmol m⁻² s⁻¹, 400 ppm CO₂ (reference side), 25°C leaf temperature, 55% humidity, 500 μmol s⁻¹ flow rate. The CO₂ response curves of CO₂ assimilation rate were measured at stepwise increases of CO₂ from 0 to 1600 ppm in 3-min intervals. A multi-phase flash of 10,000 μmol m⁻² s⁻¹ (ramp 25%) was applied to leaves at the end of each interval to transiently close all PSII reaction centres and monitor the effective quantum yield of PSII, Y(II) (Genty et al., 1989). The maximum carboxylation rate allowed by Rubisco (V_{cmax}) and the rate of photosynthetic electron transport (J) were obtained by fitting the CO₂ response curves of CO₂ assimilation using the routine of Sharkey et al. (2007). V_{cmax} was estimated at $C_i < 400$ μbar, and J was estimated at C_i between 400 and 800 μbar. Mesophyll conductance to CO₂ of 0.5 mol m⁻² s⁻¹ bar⁻¹, previously determined for tobacco (Clarke et al., 2022), was used for the fitting.

2.5 | Field experiments

The plants were grown as described in López-Calcano et al. (2019), with a methodology broadly analogous to that used commercially for tobacco. Two field sites were used: Mercedita, Puerto Rico, USA (18.004° N, 66.517° W) and the University of Illinois Energy Farm, Illinois, USA (40.062° N, 88.208° W). The field sites were prepared as described by Kromdijk et al. (2016). The same randomised block design was used in both experiments (Figure S6). Each block contained all five genotypes in five rows of four plants per genotype. The plants were grown in rows spaced 30 cm apart, with the outer boundary being a WT border. Two rows of WT borders surrounded the entire experimental site. The plants were irrigated when required using rain towers. Seeds were germinated in growth cabinets and at 12 days post-germination, moved to Transplant hydroponic trays (GP009, Speedling Inc.) and grown in the glasshouse for 20 days before being moved to the field. The plants were allowed to grow in the field until flowering (approximately 30 days). In the field, gas-exchange and fluorescence parameters were recorded using a portable infrared gas analyser LI-6400 (LI-COR Biosciences) with a 6400-40 fluorometer head unit as described in López-Calcano et al. (2020).

2.6 | Electrochromic shift and q_E

The electrochromic shift signal (ECS) was monitored as the Δ550–515 nm absorbance change, and the q_E signal was recorded at

535 nm as described in Wilson et al. (2021) using the Dual-PAM-100 (Heinz Walz) equipped with the P515/535 emitter-detector module (Heinz Walz) and coupled to the GFS-3000 gas-exchange unit with the Dual-3010 gas-exchange cuvette (Heinz Walz). After 40 min of dark adaptation, a single turnover flash was first applied to record the ECS_{ST} value. After that, the leaf was subjected to 3 min light/3 min dark intervals with red actinic light of stepwise increasing irradiance from 60 to 1500 μmol m⁻² s⁻¹. The proton-motive force (pmf) was estimated from the amplitude of the rapid ECS decay upon the light-to-dark shift normalised for ECS_{ST}. The proton conductivity of the thylakoid membrane (g_{H^+}) was calculated as the inverse time constant of the first-order exponential ECS decay (Kramer & Crofts, 1989).

2.7 | Light-induced fluorescence transients

The fast repetition rate (FRR) method was used to analyse electron transport rates from the LIFT measurements (Kolber et al., 1998). We used a commercial terrestrial LIFT-REM fluorometer (https://soliense.com/LIFT_Terrestrial.php) to apply 300 short-excitation flashlets (470 nm, 1.6 μs duration), each separated by a 2.5-μs dark interval, in a saturation sequence to gradually reduce the PSII acceptor side and PQ pool. The excitation power was sufficient to reduce Q_A to more than 90% while minimising electron flow to the PQ pool. After this saturation sequence, a relaxation sequence of 90 flashlets was applied with exponentially increasing dark intervals to allow oxidation of the PSII acceptors and PQ pool. Four of these fluorescence transients were captured, averaged and fitted with the FRR model at 5 s intervals. Examples of obtained Chl fluorescence transients are shown in Figure S5. The Q_A redox state, the relative oxidation status of the PQ pool and time constants of electron transport, Tau1 (PSII to PQ) and Tau2 (PQ to PSI), were calculated from the transients using the FRR model (<https://soliense.com/documents/LIFT-FRR%20assessment%20of%20PQ%20pool%20size.pdf>) as described in detail in Osmond et al. (2022).

The leaf was clipped to a custom-made chamber of LI-6400 of approximately 20 cm², which allowed for accurate and reproducible positioning of the leaf with respect to the light sources as well as for control of CO₂ and humidity (400 ppm CO₂ on the reference side, 25°C leaf temperature, 55% humidity, 700 μmol s⁻¹ flow rate). After 10 min of dark adaptation, a leaf was placed in the chamber and measured in darkness, followed by a far-red illumination (735 nm) at 200 μmol m⁻² s⁻¹, monitored with an SKP-216-R 550–750 nm sensor and light meter (Skye Instruments), from an LED lamp to excite PSI. Red actinic light (627 nm) at 400 μmol m⁻² s⁻¹ was provided by an SL-3500 C LED light source (PSI, Drasov, Czech Republic) and monitored with an LS-C mini-quantum sensor and ULM-500 light meter (Heinz Walz).

2.8 | Thylakoid isolation and chlorophyll analysis

Plants were dark-adapted for 12 h prior to thylakoid isolation in order to metabolise excess starch. All steps were performed in minimal light and at 4°C. One to two fully expanded leaves without the midrib were

briefly ground in a standard kitchen blender in ice-cold grinding buffer (50 mM 2-[N-morpholino]ethanesulfonic acid [MES]-NaOH, 5 mM MgCl_2 , 10 mM NaCl, 400 mM sorbitol, 0.2% ascorbate, 0.2% bovine serum albumin, 1% polyvinylpyrrolidone [PVPP], pH 6.5) supplemented with 0.5 ml L^{-1} protease inhibitor cocktail (Sigma-Aldrich). The material was filtered through two layers of Miracloth (Merck Millipore) and centrifuged at 3000 g and 4°C for 5 min. The pellet was resuspended in shock buffer (50 mM MES-KOH, pH 6.5). After the centrifugation (3000 g , 4°C, 5 min) the pellet was resuspended in resuspension buffer (50 mM MES-NaOH, 3.5 mM MgCl_2 , 7 mM NaCl, 500 mM sorbitol, pH 6.5). After the final centrifugation (3000 g , 4°C, 5 min), the pellet was resuspended in resuspension buffer supplemented with 20% glycerol at approximately 2–4 (mg Chl) ml^{-1} . The Chl ($a + b$) content was determined in 80% acetone buffered with 2.5 mM of 4-(2-hydroxyethyl)-1-piperazineethanesulfonic acid (pH 7.4) according to Porra et al. (1989).

2.9 | Spectroscopic CytF assay

The assay was performed in dim lab light, as in Anderson et al. (1997). Briefly, two identical thylakoid samples (1.1 ml each) containing 150 μM Chl ($a + b$) were prepared in measuring buffer (50 mM K_2HPO_4 pH 6.5, 0.33 M sorbitol, 1 mM MgCl_2 , 1 mM MnCl_2 , 2 mM ethylenediaminetetraacetic acid [EDTA], 1% Triton X-100). The samples were vortexed and briefly centrifuged to remove starch. The samples were scanned at 580–520 nm in a split-beam spectrophotometer (V-650, Jasco) to determine the baseline (three scans at 0.2 nm interval, 100 nm min^{-1}). Subsequently, the reference cuvette was supplemented with 0.6 mM Na-ferricyanide and the sample cuvette with 0.6 mM hydroquinone. After 90-s incubation, the samples were scanned again, and the resulting difference spectrum was used for CytF quantification using the reported extinction coefficient of 17.7 $\text{cm}^2 \text{mmol}^{-1}$ (Bendall et al., 1971). The spectra were corrected for non-linearity of the baseline using the isosbestic points at 542.5 nm and 565 nm.

2.10 | Blue Native-PAGE, SDS-PAGE and western blotting

Thylakoid complexes were separated using Blue Native-PAGE, according to Ermakova et al. (2019). For SDS-PAGE, leaf discs of 0.5 cm^2 were ground in 0.5 ml of ice-cold sample buffer (100 mM trisaminomethane [Tris]-HCl, pH 7.8, 25 mM NaCl, 20 mM EDTA, 2% w/v sodium dodecyl sulfate [SDS], 10 mM dithiothreitol, 1% w/v PVPP and 2% v/v protease inhibitor cocktail) using glass homogenizers. The leaf extracts were incubated for 10 min at 65°C and then centrifuged (4°C, 1 min, 12,000 g). The clear supernatants were supplemented with 4× SDS-loading buffer (200 mM Tris-HCl, pH 6.8, 0.8% w/v SDS, 40% glycerol, 50 mM EDTA, 10% β -mercaptoethanol, 0.08% bromophenol blue), incubated at 65°C for 10 min and loaded on leaf area basis on pre-cast polyacrylamide gels (Nu-PAGE 4–12% Bis-[2-hydroxyethyl]-amino-tris[hydroxymethyl]-methane [Bis-Tris] gel, Invitrogen, Life Technologies Corporation). The gels were run in

running buffer (50 mM MES, 50 mM Tris, 0.1% w/v SDS, 20 mM EDTA, pH 7.3) at a constant voltage of 150 V.

SDS and Blue Native gels were incubated for 10 min in a Bicine-Bis-Tris transfer buffer (25 mM Bicine, 25 mM Bis-Tris, 0.1 mM EDTA, 20% MeOH, pH 7.2) and a Tris-glycine transfer buffer (25 mM Tris, 192 mM glycine, 20% MeOH, pH 8.3), respectively. The proteins were transferred onto a nitrocellulose membrane using a semi-dry system (BioRad, Hercules, CA, USA) according to the manufacturer's protocol. The quality of the transfer and homogenous loading was assessed using ponceau stain. The membranes were probed with antibodies against various photosynthetic proteins in a dilution recommended by the producer: Rieske (AS08 330, Agrisera), CytF (Price et al., 1995), PC (Agrisera, AS06 141), PsaB (Agrisera, AS10 695), D1 (Agrisera, AS10 704), AtpB (Agrisera, AS05 085), Lhcb2 (Agrisera, AS01 003), PsbS (Agrisera, AS09 533), RbcL (Martin-Avila et al., 2020). Secondary goat anti-rabbit horse radish peroxidase-conjugated antibody (Biorad) was detected using a Western lightning Ultra chemiluminescence kit (Perkin Elmer). Quantification of the signals was performed using ImageJ software. The linearity of the western blot signals and the ponceau stain is plotted in Figure S3.

2.11 | Statistical analysis

Type 1 analysis of variance (ANOVA) with Tukey HSD or two-tailed, heteroscedastic Student t test was performed to test the relationship between mean values for transgenic and control plants. For field studies, a linear mixed effect model with type 2 ANOVA was used to identify differences in the curves while accounting for (random) block effects. The lmer function of the lme4 R package was used, followed by a contrast analysis (lsmeans, from emmeans R package). Details of tests and replicates are provided in the figure legends.

3 | RESULTS

3.1 | Generation of transgenic tobacco plants

Using *Agrobacterium*-mediated leaf transformation, *N. tabacum* was transformed with a construct for Rieske-OE (Figure S1). From 20 independent lines generated, 9 lines with a single gene insertion were screened for transgene expression, and transcripts of the transgenic *petC* were detected in 8 of those lines in the T_1 generation (Figure 1). Homozygous plants were selected from the T_1 progenies of lines R13, R17, R20, R25 and R26. The progenies of the homozygous plants were used in all further analyses.

3.2 | Cytochrome b_6f is functional in Rieske-OE plants

Rieske-OE plants were analysed for Cyt b_6f abundance and activity. To estimate the content of Cyt b_6f , we separated thylakoid protein complexes from wild type (WT) and Rieske-OE plants by Blue Native-

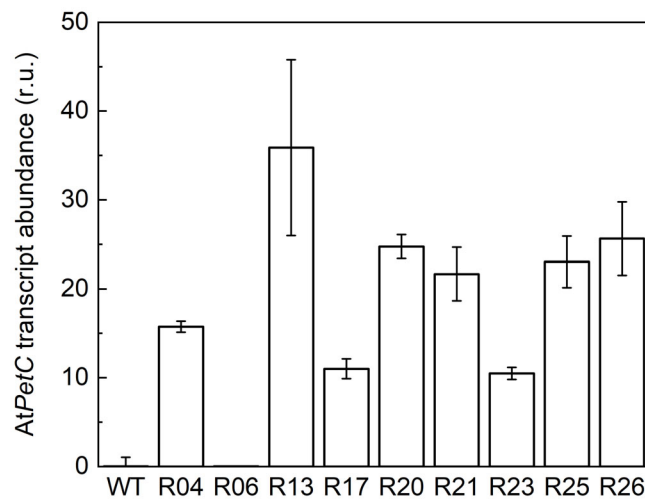


FIGURE 1 Relative *AtPetC* transcript abundance as fold of *NtActin* in homozygous T_1 plants and WT plants. The individuals used in this analysis generated the T_2 seeds used for the phenotyping experiments presented below. Mean \pm SD, $n = 3$ technical replicates

PAGE and detected the complex using the Rieske antibody (Figures 2 and S2). A band matching the size of a dimeric *Cytb₆f* complex of approximately 400 kDa was recognised (Kügler et al., 1997). Relative quantification showed a 20%–60% increased abundance of *Cytb₆f* in all lines (significant in lines R13 and R17) (Figures 2 and S2). To verify the functionality of the complex in Rieske-OE plants, we used the reduced-oxidised (hydroquinone minus ferricyanide) difference spectroscopy assay of CytF, one of the redox cofactors of *Cytb₆f*. The absorption peak of the characteristic alpha band at 554 nm was used to quantify the amount of CytF in the sample using the extinction coefficient of $17.7 \text{ cm}^2 \text{ mmol}^{-1}$ (Figure 3A). All lines, except for R13, displayed a 10%–30% increase of CytF activity, significant for lines R17, R20 and R26 (Figure 3B). WT CytF activity remained constant between different batches of plants (Figure S4).

Next, we selected lines R13, R17, R25 and R26 to analyse the abundance of photosynthetic proteins in leaf extracts by immunoblotting with specific antibodies (Figure 4). A significant, near twofold increase of Rieske abundance was confirmed in all lines on a leaf area basis. No changes in abundance of D1 (PSII), PsaB (PSI), nor AtpB (ATP synthase) were detected in any transgenic lines, suggesting an unaltered abundance of the corresponding thylakoid complexes. The content of the large subunit of Rubisco (RbcL) and PsaB did not differ between the WT and Rieske-OE plants. Interestingly, the soluble electron carrier between *Cytb₆f* and PSI, plastocyanin (PC), and the Lhcb2 subunit of the light-harvesting complex II (LHCII) displayed an opposite trend between the lines, with a significant decrease of PC in lines R25 and R26 and a significant decrease of Lhcb2 in lines R13 and R17.

3.3 | Overexpression of Rieske changes LIFT

To analyse the function of *Cytb₆f* in Rieske-OE plants in vivo, we studied electron transport rates by the LIFT technique using the FRR

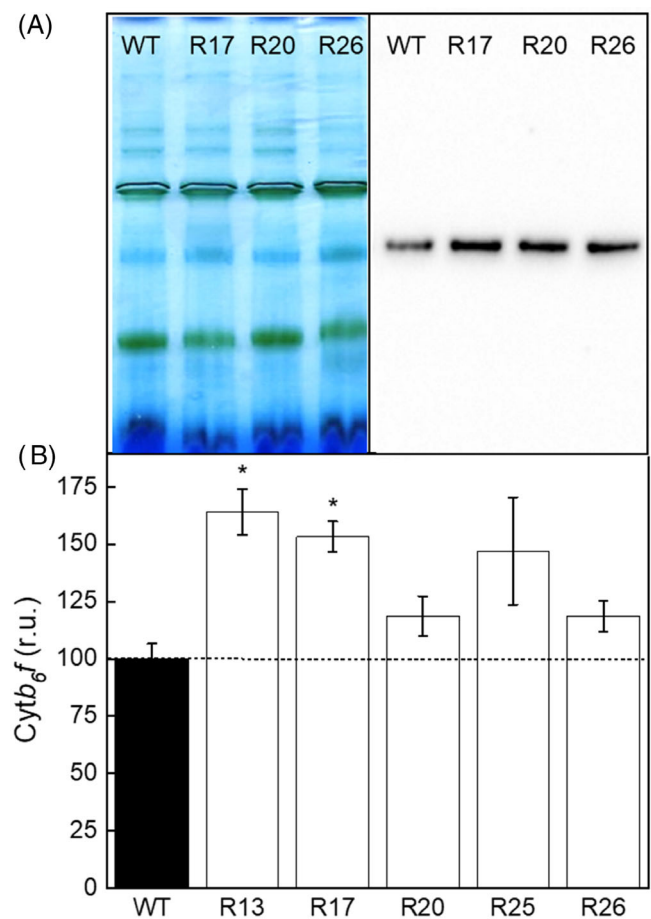


FIGURE 2 Immunodetection of cytochrome *b₆f* complex from the thylakoid membranes of WT and Rieske-OE plants. (A) Blue Native-PAGE of the thylakoid protein complexed followed by the western blotting with Rieske antibodies (left and right panels, respectively). A sample of 10 μg Chl (*a + b*) of each sample was loaded. Additional gel and blot images of all lines tested are shown in Figure S2. (B) Relative quantification of the blots. Mean \pm SE, $n = 3$ biological replicates. Asterisks indicate statistically significant differences between transgenic lines and WT (Tukey test, $p < 0.05$).

method (Kolber et al., 1998). This near-remote sensing method (0.6–40 m) is finding increasing applications in phenotyping of photosynthetic electron transport kinetics in the field (Keller, Matsubara, et al., 2019; Keller, Vass, et al., 2019). The advantages of this method are fast time resolution and minimally intrusive in situ approach via the use of sub-saturating short excitation pulses ('flashlets') that exert minimal changes to the redox state of electron carriers as opposed to high intensity flashes used in pulse amplitude modulation (PAM) fluorescence technique. Using recently developed LIFT protocols for laboratory analysis of plants (Osmond et al., 2019; Osmond et al., 2022), we assessed in vivo activity of *Cytb₆f* in tobacco. LIFT-FRR method allows for real-time monitoring of F_V/F_M (reporting on the redox states of Q_A , the primary quinone acceptor of PSII), the redox state of the plastoquinone (PQ) pool and electron transport rates from PSII to PQ pool (Tau1) and from PQ pool to PSI (Tau2) (Osmond et al., 2019; see also under Photosynthetic signatures at https://soliense.com/LIFT_Method.php). The Q_A is first gradually reduced by flashlets at

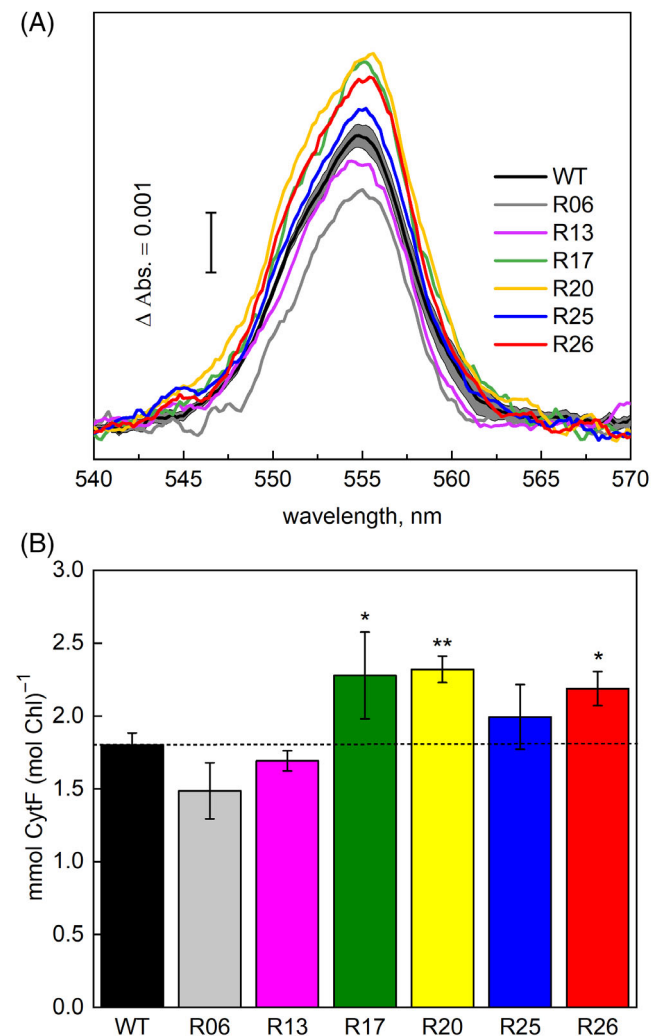


FIGURE 3 Quantification of CytF content in the thylakoid membranes of WT and Rieske-OE plants. (A) The reduced-minus-oxidised CytF spectra. Traces are average of three to eight biological replicates; SE range is shown for the WT trace. (B) Relative abundance of CytF calculated from the 554 nm peak. Mean \pm SE, $n = 8$ biological replicates for WT, $n = 3$ for transgenic lines. Asterisks indicate statistically significant differences between transgenic lines and WT (Tukey test, $p < 0.05$).

microsecond intervals until the fluorescence signal is saturated (300 flashlets). This is immediately followed by a Q_A re-oxidation flash routine, during which the time between the flashlets is exponentially increased to allow for graduate re-oxidation (90 flashlets). Each flashlet cycle, i.e., the excitation and re-oxidation flashlets (390 in total), yields ~ 300 ms chlorophyll (Chl) fluorescence transients (Figure S5) that are fitted by the FRR model to derive Chl fluorescence parameters.

Illumination of the dark-adapted tobacco leaves with far-red light caused an increase in Tau1, indicating a slower electron transport from PSII to the PQ pool, as well as a more oxidised PQ pool and a decrease in Tau2, indicating faster electron transport from the PQ pool to PSI (Figure 5). The effect of far-red on Tau1 remained throughout the FR illumination while Tau2 gradually

returned to the level observed in darkness, showing a slow-down of electron transport to PSI. These observations were consistent with an operation of far-red light-driven cyclic electron flow and showed no difference between the WT and transgenic plants. Next, red actinic light of $400 \mu\text{mol m}^{-2} \text{s}^{-1}$ was added on top of the far-red illumination (indicated by arrows in Figure 5), which induced a rapid reduction of Q_A (seen as a drop in F_V/F_M) and PQ pool, followed by a gradual re-oxidation until it reached a quasi-steady-state level after approximately 3 min. Tau1 and Tau2 displayed reproducible transients with one or two peaks (i.e., slower electron transport), respectively, before reaching a steady-state. Line R17 and R26 displayed significantly decreased Tau2 values, corresponding to faster electron transport rates between the plastoquinone pool and PSI. Line R25 showed a similar trend of F_V/F_M as the other lines, although not significant, but the Tau2 values were also significantly lower in this line. Interestingly, initial differences in Q_A and PQ pool oxidation between WT and transgenic lines, seen at the beginning of actinic light illumination, were often reduced by the end of the illumination period. Collectively, these results suggested that Rieske-OE lines maintained transiently more oxidised PQ pool and Q_A upon changes in irradiance, likely, due to the increased Cytb₆f activity.

3.4 | Thylakoid membrane energisation in Rieske-OE plants

Next, we assessed pmf established in leaves of WT and Rieske-OE plants at different irradiance by monitoring the dark interval relaxation kinetics of the ECS (Figure 6A). Lines R25 and R26 showed slightly increased pmf at $1000 \mu\text{mol m}^{-2} \text{s}^{-1}$ and above while line R17 did not differ from the WT. No differences in the proton conductivity of the thylakoid membrane (g_{H^+}) were observed between the genotypes suggesting that activity of the chloroplast ATP synthase was not altered in Rieske-OE plants (Figure 6B). Absorption changes at 535 nm upon the illumination largely account for the q_E formation in response to acidification of the lumen (Wilson et al., 2021). Upon the shift from dark to $400 \mu\text{mol m}^{-2} \text{s}^{-1}$, all three measured transgenic lines established q_E significantly more rapidly than WT (Figure 6C), consistent with a faster build-up of ΔpH in plants with increased Cytb₆f activity.

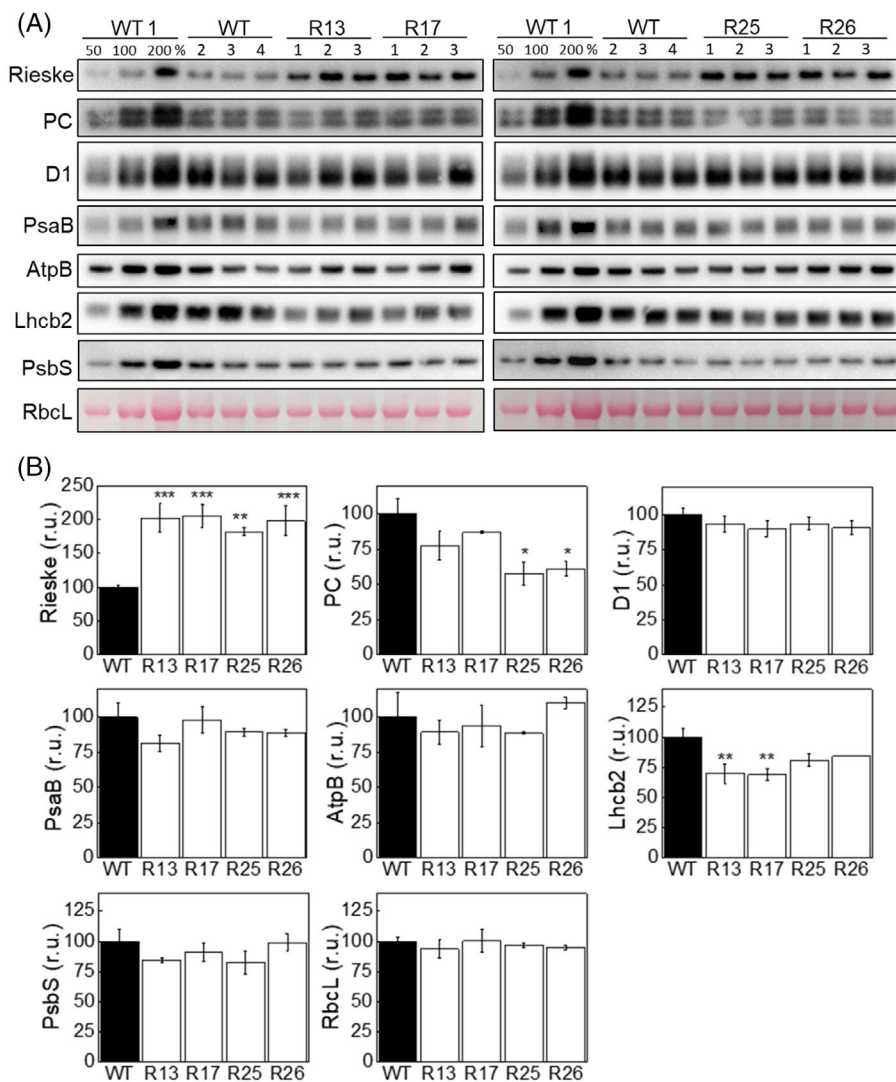
3.5 | Gas exchange and electron transport rates of Rieske-OE plants

We studied the effects of increased Cytb₆f activity in tobacco on the net CO_2 assimilation rate and effective quantum yield of PSII, Y(II), at different CO_2 partial pressures. No significant changes in either parameter were observed in Rieske-OE lines compared to WT (Figure 7). The maximum carboxylation rate allowed by Rubisco (V_{cmax}) and the rate of photosynthetic electron transport based on NADPH requirement (J) obtained by fitting the CO_2 response curves

FIGURE 4 Abundance of photosynthetic proteins in leaves of WT and Rieske-OE plants.

(A) Immunodetection of Rieske, plastocyanin (PC), D1 subunit of PSII, PsaB subunit of PSI, AtpB subunit of ATP synthase, Lhcb2 subunit of LHCII and PsbS in leaf protein extracts loaded on leaf area basis. The quantity of the large subunit of Rubisco (RbcL) was estimated from Ponceau stained membranes immediately after transfer. A titration series of one of the WT samples (WT1) was used for relative quantification.

(B) Quantification of immunoblots relative to WT. mean \pm SE, $n = 4$ biological replicates for WT, $n = 3$ for transgenic lines. Asterisks indicate statistically significant differences between transgenic lines and WT (Tukey test, * $p < 0.05$, ** $p < 0.01$, *** $p < 0.001$).



of CO_2 assimilation showed no differences between the genotypes (Table 1). The leaf mass per area and total leaf Chl content were not altered in the transgenic lines compared to WT (Table 1). There was a slight increase in the Chl a/b ratio in lines R13 and R17, which could reflect the altered abundances in the Lhcb2 amounts seen in those lines (Figure 4).

3.6 | Field trials

To study the effects of increased *Cytb₆f* activity on CO_2 assimilation and electron transport in tobacco grown in field conditions, three Rieske-OE lines and control plants were grown to maturity in two field sites in Puerto Rico and Illinois (the randomised design of field trials is shown in Figure S6). When grown in Puerto Rico, two Rieske-OE lines showed significantly increased CO_2 assimilation rates compared to control plants at light intensities above $900 \mu\text{mol m}^{-2} \text{s}^{-1}$ (Figure 8A,C,E). Transgenic plants had similar Y(II) to control plants, and only line R26 showed higher C_i/C_a (the ratio of intercellular to

ambient CO_2 partial pressures) above $900 \mu\text{mol m}^{-2} \text{s}^{-1}$, suggesting that the detected increases in assimilation were not related to improvements in electron transport, but differences in stomatal conductance. Indeed, all lines showed significantly increased stomatal conductance during the light curves (data not shown). The Illinois field experiments revealed no changes between the genotypes in CO_2 assimilation, Y(II) or C_i/C_a at any irradiance (Figure 8B,D,F). Regarding responses to different CO_2 partial pressures, CO_2 assimilation and Y(II) did not consistently differ between transgenic and control plants grown in Illinois (Figure S7), with only one line (R26) showing significantly increased CO_2 assimilation rates and no differences in Y(II) were seen in any line.

4 | DISCUSSION

Improving photosynthesis is one of the promising routes to increase the biomass and yield of crop plants (Walter & Kromdijk, 2022). However, better understanding of the mechanisms and consequences of

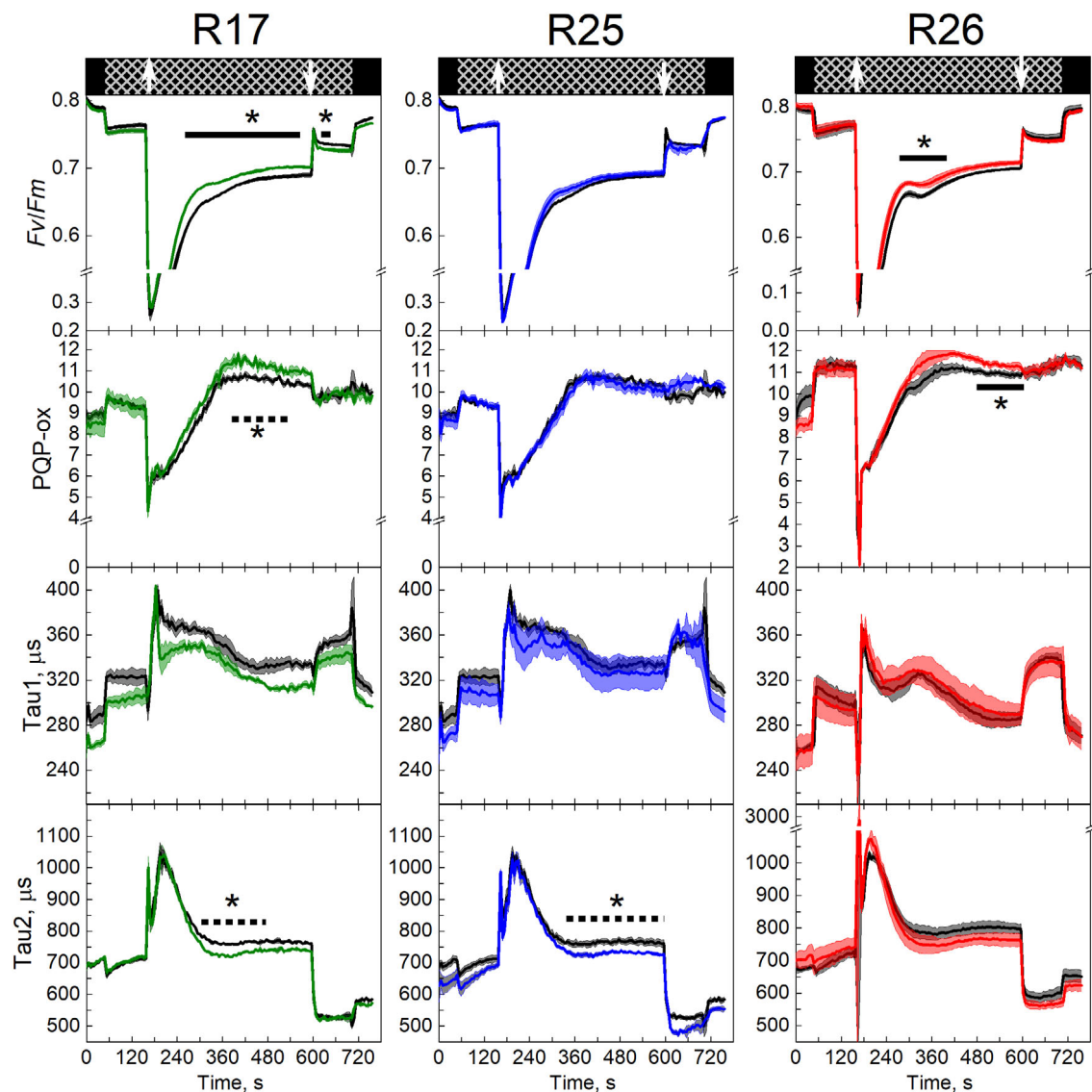


FIGURE 5 Electron transport parameters of WT (black traces) and Rieske-OE lines R17, R25 and R26 derived from the light-induced fluorescent transients measurements. The upper panels indicate background illumination during the measurement: black = darkness; hatched = far-red light of $200 \mu\text{mol m}^{-2} \text{s}^{-1}$; arrows indicate the onset and offset of red actinic light of $400 \mu\text{mol m}^{-2} \text{s}^{-1}$. F_v/F_m , oxidised Q_A sites; PQP_ox, oxidation state of the plastoquinone pool; Tau1, electron transport rate from PSII to the plastoquinone pool; Tau2, electron transport rate from the plastoquinone pool to PSI. Mean \pm SE, $n = 3$ biological replicates for transgenic lines, $n = 4$ for WT. Asterisks indicate statistically significant differences between transgenic lines and WT over a time period (Tukey test, $p < 0.05$). A solid line indicates that all data points were significantly different, a broken line indicates that at least 50% of the data points were significantly different.

increasing the efficiency of photosynthetic reactions in different model species is required to accelerate the implementation of these strategies into crops. Overexpression of Rieske previously showed promising results in the model species *A. thaliana* producing higher electron transport and CO_2 assimilation rates as well as increased biomass accumulation and seed yield (Simkin et al., 2017). Here we tested whether those results could be translated into tobacco, an agronomic crop and a model for other Solanaceae crops, like tomato and potato.

Overexpression of Rieske in tobacco increased the abundance of functional Cytb_6/f . Previous works showed that plants overexpressing

Rieske had higher leaf content of other subunits of the complex (Simkin et al., 2017) or more Cytb_6/f (Ermakova et al., 2019). Here we expand on those results and demonstrate that leaves of Rieske-OE tobacco plants contain significantly more of functionally active Cytb_6/f using the CytF activity assay. While the total abundance of Rieske in leaves of transgenic plants was on average double compared to WT, we detected an average of 40% increase of Cytb_6/f abundance (Figure 2). These results suggest that assembly of the complex was likely limited either by integration of Rieske into the thylakoid membrane (Molik et al., 2001) or by the availability of other subunits. Furthermore, transgenic plants showed only a 20% increase in CytF

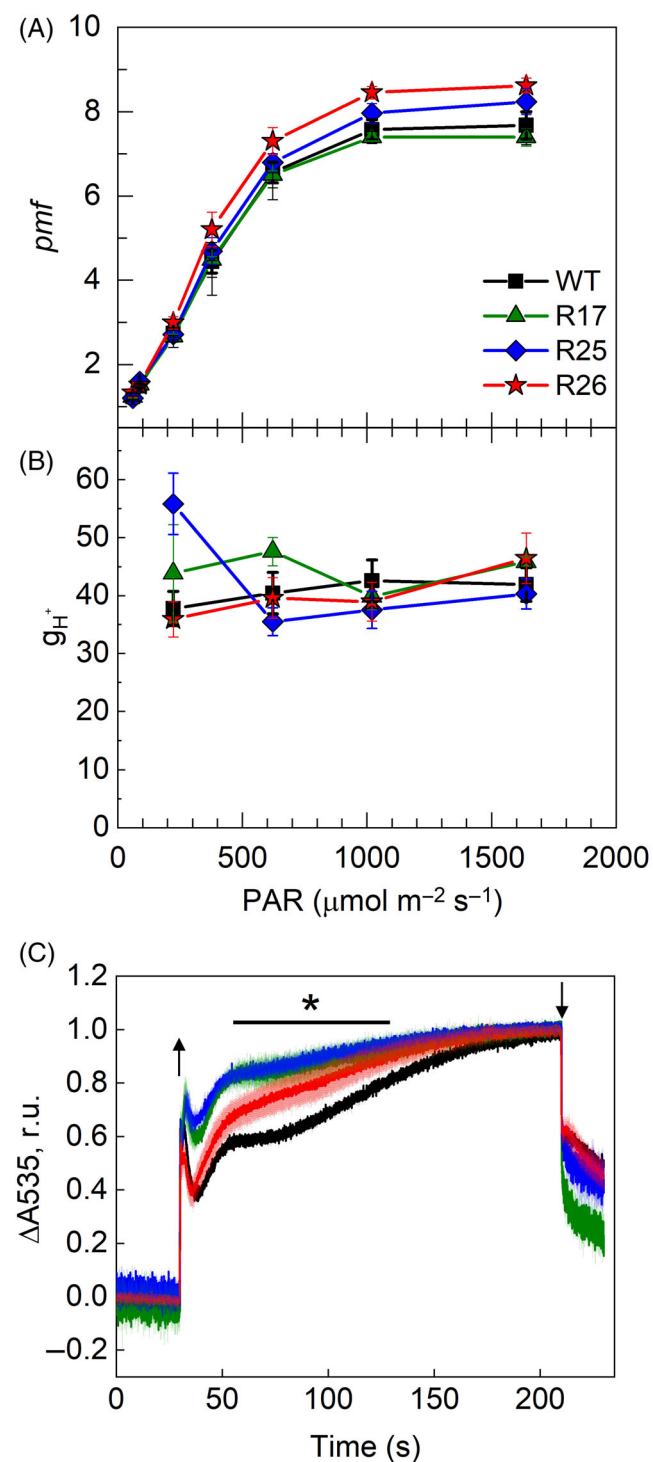


FIGURE 6 Analysis of the thylakoid membrane energisation in WT and Rieske-OE plants. (A, B) Proton motive force (pmf) and proton conductivity of the thylakoid membrane (g_{H^+}) at different irradiances. Mean \pm SE, $n = 4$ biological replicates. (C) Changes in absorbance at 535 nm during the dark-light-dark transitions. Traces were normalised to 0 in the beginning of illumination ($400 \mu\text{mol m}^{-2} \text{s}^{-1}$, arrow up) and to 1 in the end of illumination (arrow down) to facilitate comparison of the kinetics. Traces are average of three biological replicates, SE is shown as a lighter shade. Asterisks indicate statistically significant differences between transgenic lines and WT (Tukey test, $p < 0.05$). The solid line indicates the time frame of significant differences between the lines.

activity compared to control plants (Figure 3). It is currently thought that $Cytb_6f$ assembly starts with the membrane insertion of cytochrome b_6 and subunit IV and their dimerisation, followed by the insertion of CytF and Rieske (Hasan et al., 2013; Schöttler et al., 2015). Thus, $Cytb_6f$ complexes immunodetected with Rieske antibody should already contain CytF (Figures 2 and 3). However, it is conceivable that some (virtually) fully assembled complexes are inactive in electron transport, for example, if haeme-less CytF is assembled (Mould et al., 2001). Further research is required to identify whether co-overexpression of Rieske with other subunits or regulatory proteins is required to ensure the functionality of all assembled complexes.

Rieske-OE plants reached an increased $Cytb_6f$ activity in vivo. The first line of evidence came from the LIFT measurements. Plants overexpressing Rieske had more oxidised Q_A than WT, meaning that their PSII centres were kept more open after the onset of actinic light (Figure 5). PQ pool was also more oxidised in Rieske-OE lines, and the rates of electron transport from PSII to PQ pool (τ_{11}) and from PQ pool to PSI were faster, compared to WT. These results suggested

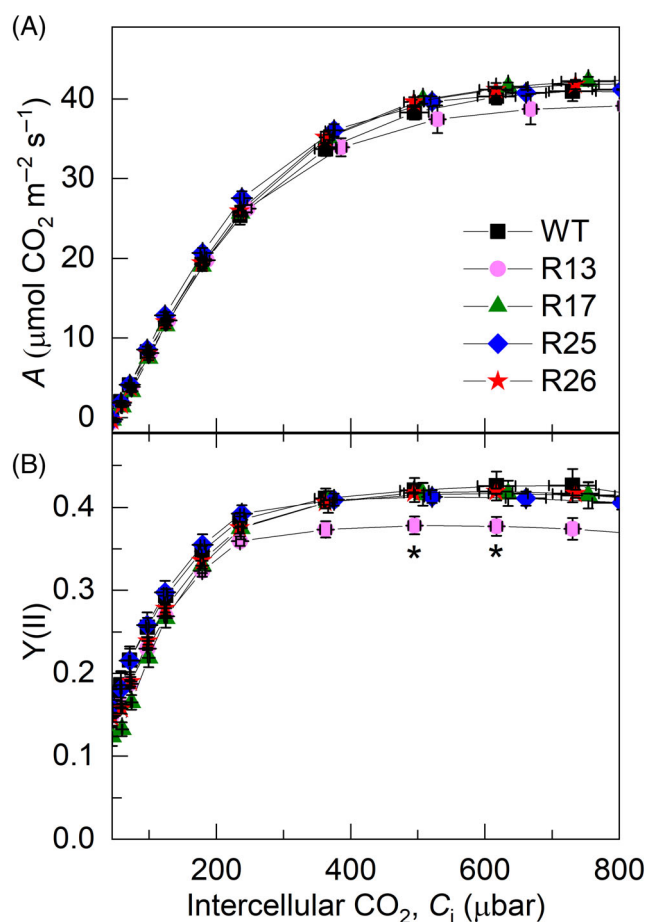


FIGURE 7 Photosynthetic properties of WT and Rieske-OE tobacco plants grown in controlled conditions. (A) CO_2 assimilation rate, A ; (B) the effective quantum yield of PSII, $Y(II)$. Measurements were performed at $1500 \mu\text{mol m}^{-2} \text{s}^{-1}$ and different CO_2 partial pressures. Mean \pm SE, $n = 3$ biological replicates for Rieske-OE lines, $n = 6$ for WT. Asterisks indicate statistically significant differences between transgenic lines and WT (Tukey test, $p < 0.05$).

TABLE 1 Gas exchange and biochemical properties of WT and Riese-OE tobacco plants

Parameter	WT	R13	R17	R25	R26
LMA, g (dry weight) m ⁻²	28.3 ± 1.7	30.8 ± 1.5	25.5 ± 0.7	28.1 ± 1.7	31.8 ± 1.5
Chl (a + b), mmol m ⁻²	0.61 ± 0.03	0.60 ± 0.04	0.56 ± 0.04	0.57 ± 0.04	0.61 ± 0.03
Chl a/b	4.26 ± 0.02	4.38 ± 0.05*	4.45 ± 0.03*	4.36 ± 0.043	4.30 ± 0.02
V _{cm_{max}} , μmol m ⁻² s ⁻¹	147 ± 1.2	148 ± 7.0	143 ± 5.7	160 ± 11.8	152 ± 1.5
J, μmol m ⁻² s ⁻¹	204 ± 4.7	198 ± 10.3	212 ± 1.8	206 ± 2.6	212 ± 3.6
J/V _{cm_{max}}	1.39 ± 0.03	1.34 ± 0.02	1.48 ± 0.05	1.42 ± 0.06	1.40 ± 0.02

Note: Samples were collected from the leaf area used for gas exchange measurements presented in Figure 7. Mean ± SE, n = 3 biological replicates.

Asterisks indicate statistically significant differences between transgenic lines and WT (Tukey test, p < 0.05).

Abbreviations: LMA, leaf mass per area; J, rate of electron transport based on NADPH requirement; V_{cm_{max}}, maximum carboxylation rate allowed by rubisco.

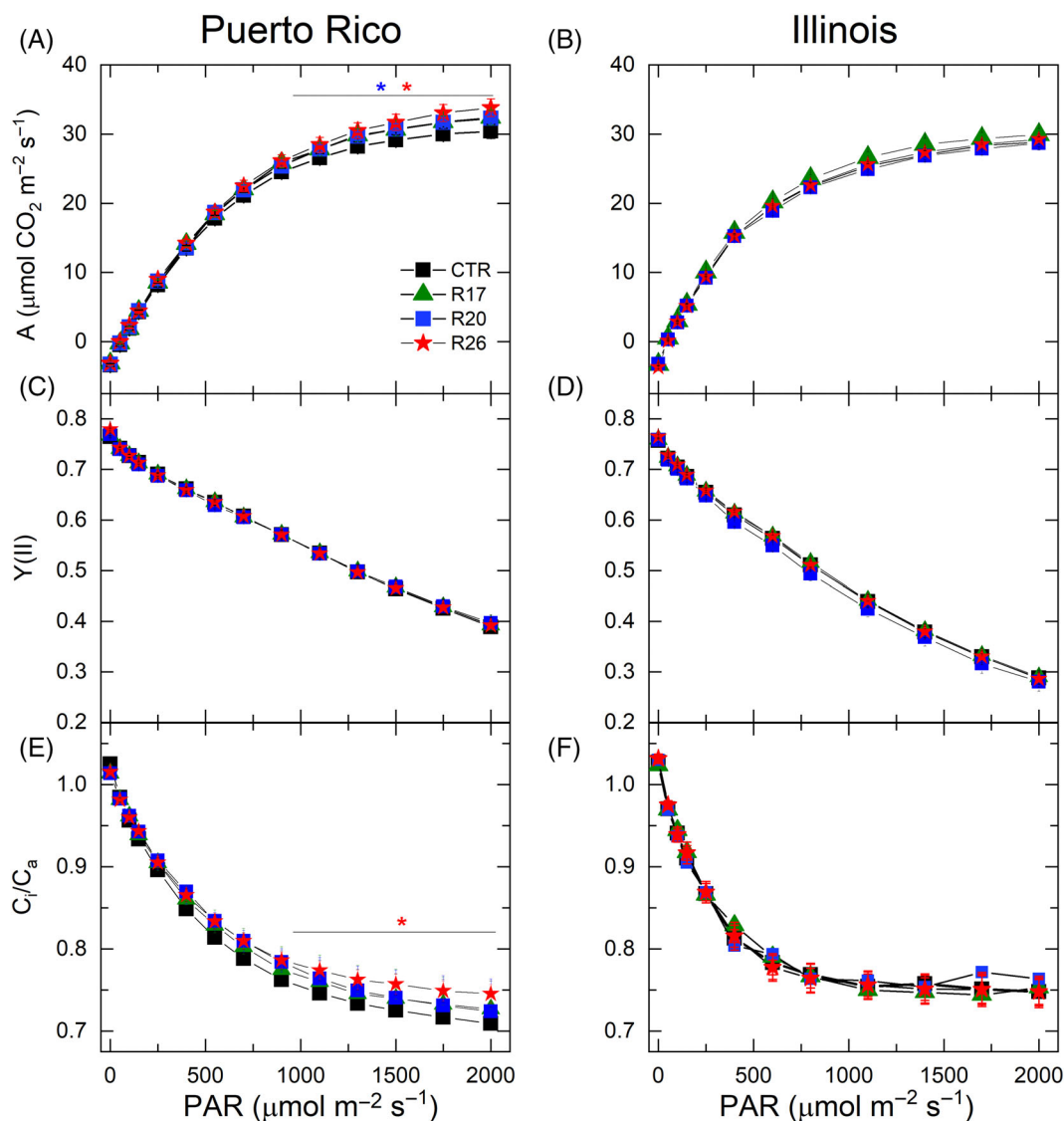


FIGURE 8 Light responses of photosynthetic parameters measured at ambient CO₂ from control and Riese-OE tobacco plants grown in the field. (A, C, E) Puerto Rico trials; (B, D, F) Illinois field trials. (A and B) CO₂ assimilation rate, A; (C and D) the effective quantum yield of PSII, Y(II); (E and F) the ratio of intercellular and ambient CO₂ partial pressures, C_i/C_a. The control group (CTR) contained WT and azygous plants. Mean ± SE, n = 18 biological replicates for CTR in Puerto Rico, n = 24 for CTR in Illinois, n = 9 for transgenic lines in Puerto Rico, n = 12 for transgenic lines in Illinois. Asterisks indicate statistically significant differences between transgenic lines and WT (linear mixed-effects model and type II ANOVA, p < 0.05).

that an increased abundance of *Cytb₆f*, relative to PSI and PSII (Figure 4), could accelerate intersystem electron transfer reactions and keep the PQ pool transiently more oxidised. The second line of evidence for the increased in vivo *Cytb₆f* activity in Rieske-OE tobacco plants came from the absorbance measurements at 535 nm, which reflect both zeaxanthin formation and the modification of the LHCII induced by PsbS (Wilson et al., 2021). Since both components are sensitive to the lumenal pH, the rise of the 535 nm signal in illuminated leaves informs about the kinetics of ΔpH build-up across the thylakoid membrane, largely mediated by *Cytb₆f*. Three Rieske-OE lines showed a faster rise of 535 nm signal suggesting a faster acidification of the lumen, which is consistent with the increased abundance of *Cytb₆f*. However, *pmf*, representing the total energisation of the thylakoid membranes, which is a sum of ΔpH and $\Delta\psi$ (the membrane potential), sampled after 3 min of illumination, did not differ between Rieske-OE and WT plants (Figure 6). Therefore, the kinetics of the 535 nm signal indicated that electron transport, initially increased in transgenic plants, was subsequently slowed down to a WT-level by the end of 3-min illumination period. Similar trends were observed in the redox states of Q_A and PQ pool measured by LIFT: the largest differences between transgenic and WT plants were observed 1–2 min after the onset of illumination while, towards the end of the 3-min illumination, all lines were approaching similar values (Figure 5).

The observed transient increases in *Cytb₆f* activity were possible because the formation of q_E takes time to respond to ΔpH . NPQ is a part of the complex regulatory network that is in place to balance the activity of light and dark reactions of photosynthesis to protect the photosynthetic machinery from damaging effects of harvesting excess light energy. When the capacity of light reactions exceeds the utilisation of NADPH and ATP by the Calvin cycle, regulation of ATP synthase conductivity and cyclic electron flow helps to build up the proton gradient, activate NPQ and finally reduce electron transport rate (Avenson et al., 2005; Kanazawa & Kramer, 2002). The conserved relationship between NPQ and *pmf* would constrain the rate of electron transport, which is in line with our finding showing that the steady-state electron transport rate was not affected by the increased *Cytb₆f* activity. Thus, our results indicate that *Cytb₆f* is not the only factor controlling electron transport rate in high light and high CO_2 (Figure 7), the conditions in which electron transport is expected to limit CO_2 assimilation (Farquhar et al., 1980; von Caemmerer & Farquhar, 1981). Accordingly, the increased electron transport and CO_2 assimilation rates detected in Rieske-OE *A. thaliana* plants could not be solely attributed to the increased *Cytb₆f* activity since higher abundances of other photosynthetic complexes were also reported (Simkin et al., 2017).

In response to higher light levels, photosynthetic control exerts an additional constraint on the electron transport in Rieske-OE plants. This effect can mask changes in the intrinsic activity of *Cytb₆f*. As such, changes in *Cytb₆f* activity are expected to be most readily observed under light conditions the plant is acclimated to i.e. growth light levels. This is exactly what we observe: transient increases in *Cytb₆f* activity were only clearly resolved at light levels $400 \mu\text{mol m}^{-2} \text{s}^{-1}$, similar to growth conditions (Figures 5 and 6). We

note that under these conditions, the model of Johnson and Berry (2021) can be used to estimate the activity of *Cytb₆f* and, thus, the maximal rate of electron transport. The model assumes photosynthetic control is relaxed. That is to say, both NADP^+ and ADP/P_i are available and do not limit *Cytb₆f* activity. It is important to recognise that the maximal electron transfer rate depends on the light level used.

At higher light intensities and ambient CO_2 levels, limited CO_2 availability slows down the consumption of NADPH and ATP by the Calvin cycle, which rapidly downregulates *Cytb₆f* activity via photosynthetic control before slower regulatory processes like q_E and state transitions develop. Although the mechanism of photosynthetic control is not known, it is suggested to be an intrinsic feature of *Cytb₆f* (Malone et al., 2021). It would be interesting to explore whether there is a natural variation in the degree of control this phenomenon exerts over electron transport. Unravelling molecular mechanisms of photosynthetic control would allow optimising it for improving plant productivity.

Due to the above-mentioned limitations, increased *Cytb₆f* abundance and activity in Rieske-OE plants failed to stimulate steady-state electron transport rate in either controlled or field conditions (Figures 7 and 8). Consequently, steady-state CO_2 assimilation rates were not consistently increased in Rieske-OE lines, except for some lines grown in Puerto Rico, which, however, had an elevated CO_2 availability (Figure 8). Nevertheless, the detected transient increases in *Cytb₆f* activity suggest that Rieske-OE could be beneficial if combined with other traits stimulating downstream processes. For example, overexpression of sedoheptulose-1,7-bisphosphatase enzyme of the Calvin cycle is known to stimulate carbon assimilation (Driever et al., 2017; Lefebvre et al., 2005) and could accelerate the use of NADPH and ATP and allow higher electron transport rate in Rieske-OE plants. Simultaneous stimulation of electron transport and the Calvin cycle was previously shown to increase tobacco biomass and yield in the field (López-Calcagno et al., 2020). Finally, we have recently shown that increasing the abundance of the ATP synthase via over-expression of the *AtpD* subunit significantly upregulated photosynthetic rates in rice in high light conditions (Ermakova et al., 2022). Testing and combining targets for improving photosynthetic efficiency and deciphering molecular mechanisms of photosynthetic regulation will help to provide necessary improvements to photosynthesis crucial for improving crop productivity.

5 | CONCLUSIONS

Cytb₆f is one of the main control points limiting electron transport rate. Here we generated tobacco plants with increased Rieske content with more functional *Cytb₆f*, compared to control plants, without marked changes in abundance of other photosynthetic components. Plants with increased *Cytb₆f* abundance displayed a faster build-up of the transmembrane proton gradient and higher electron transport rates, however, only transiently. In contrast to

Rieske-OE in *Arabidopsis* (Simkin et al., 2017), steady-state rates of electron transport and CO₂ assimilation were not affected in tobacco overexpressing Rieske, pointing to differences between species. These results suggest that *Cytb₆f* is not the only factor limiting electron transport at high light and high CO₂ in tobacco.

AUTHOR CONTRIBUTIONS

Christine A. Raines, Susanne von Caemmerer, Eiri Heyno, Maria Ermakova, Patricia E. Lopez-Calcagno designed the research; Eiri Heyno, Maria Ermakova, Patricia E. Lopez-Calcagno, Russell Woodford, Kenny L. Brown, Jack S. A. Matthews, Barry Osmond performed research; Eiri Heyno, Maria Ermakova, Patricia E. Lopez-Calcagno, Russell Woodford, Barry Osmond analysed data; Eiri Heyno, Maria Ermakova and Susanne von Caemmerer wrote the paper.

ACKNOWLEDGMENTS

This study was funded by the Bill and Melinda Gates Foundation RIPE (Realizing Increased Photosynthetic Efficiency) programme. The Australian Plant Phenomics Facility supported under the National Collaborative Research Infrastructure Strategy of the Australian Government is gratefully acknowledged for the use of growth facilities and equipment. We thank Dean Price and Spencer Whitney for the gift of antibodies. We thank Z. Kolber for frequent and tireless help with LIFT. Open access publishing facilitated by Australian National University, as part of the Wiley - Australian National University agreement via the Council of Australian University Librarians.

DATA AVAILABILITY STATEMENT

The data that support the findings of this study are available from the corresponding author upon reasonable request.

ORCID

Eiri Heyno  <https://orcid.org/0000-0003-2172-0341>
 Maria Ermakova  <https://orcid.org/0000-0001-8466-4186>
 Patricia E. Lopez-Calcagno  <https://orcid.org/0000-0003-2436-8988>
 Russell Woodford  <https://orcid.org/0000-0002-6766-2274>
 Kenny L. Brown  <https://orcid.org/0000-0002-0587-2698>
 Jack S. A. Matthews  <https://orcid.org/0000-0002-7282-8929>
 Barry Osmond  <https://orcid.org/0000-0002-3569-7763>
 Christine A. Raines  <https://orcid.org/0000-0001-7997-7823>
 Susanne von Caemmerer  <https://orcid.org/0000-0002-8366-2071>

REFERENCES

- Anderson, J.M., Dean Price, G., Soon Chow, W., Hope, A.B. & Badger, M.R. (1997) Reduced levels of cytochrome *bf* complex in transgenic tobacco leads to marked photochemical reduction of the plastoquinone pool, without significant change in acclimation to irradiance. *Photosynthesis Research*, 53, 215–227.
- Avenson, T.J., Cruz, J.A., Kanazawa, A. & Kramer, D.M. (2005) Regulating the proton budget of higher plant photosynthesis. *Proceedings of the National Academy of Sciences of the United States of America*, 102, 9709–9713.
- Bailey-Serres, J., Parker, J.E., Ainsworth, E.A., Oldroyd, G.E.D. & Schroeder, J.I. (2019) Genetic strategies for improving crop yields. *Nature*, 575, 109–118.
- Bendall, D.S., Davenport, H.E. & Hill, R. (1971) Cytochrome components in chloroplasts of the higher plants. In: *Methods in enzymology*, Vol. 23. New York: Academic Press, pp. 327–344.
- Clarke, V.C., De Rosa, A., Massey, B., George, A.M., Evans, J.R., von Caemmerer, S. et al. (2022) Mesophyll conductance is unaffected by expression of *Arabidopsis* PIP1 aquaporins in the plasmalemma of *Nicotiana*. *Journal of Experimental Botany*, 73, 3625–3636.
- Colombo, M., Suorsa, M., Rossi, F., Ferrari, R., Tadini, L., Barbato, R. et al. (2016) Photosynthesis control: an underrated short-term regulatory mechanism essential for plant viability. *Plant Signaling & Behavior*, 11, e1165382.
- Driever, S.M., Simkin, A.J., Alotaibi, S., Fisk, S.J., Madgwick, P.J., Sparks, C. A. et al. (2017) Increased SBPase activity improves photosynthesis and grain yield in wheat grown in greenhouse conditions. *Philosophical Transactions of the Royal Society B: Biological Sciences* 372, 20160384.
- Engler, C., Youles, M., Gruetzner, R., Ehnert, T.-M., Werner, S., Jones, J.D. G. et al. (2014) A golden gate modular cloning toolbox for plants. *ACS Synthetic Biology*, 3, 839–843.
- Ermakova, M., Heyno, E., Woodford, R., Massey, B., Birke, H. & von Caemmerer, S. (2022) Enhanced abundance and activity of the chloroplast ATP synthase in rice through the overexpression of the *AtpD* subunit. *Journal of Experimental Botany*, erac320.
- Ermakova, M., Lopez-Calcagno, P.E., Raines, C.A., Furbank, R.T. & von Caemmerer, S. (2019) Overexpression of the Rieske FeS protein of the cytochrome *b₆f* complex increases C₄ photosynthesis in *Setaria viridis*. *Communications Biology*, 2, 314.
- Ermakova, M., Osborn, H., Groszmann, M., Bala, S., Bowerman, A., McGaughey, S. et al. (2021) Expression of a CO₂-permeable aquaporin enhances mesophyll conductance in the C₄ species *Setaria viridis*. *eLife*, 10, e70095.
- Evans, J.R. (2013) Improving photosynthesis. *Plant Physiology*, 162, 1780–1793.
- Farquhar, G.D., von Caemmerer, S. & Berry, J.A. (1980) A biochemical-model of photosynthetic CO₂ assimilation in leaves of C₃ species. *Planta*, 149, 78–90.
- Genty, B., Briantais, J.M. & Baker, N.R. (1989) The relationship between the quantum yield of photosynthetic electron-transport and quenching of chlorophyll fluorescence. *Biochimica et Biophysica Acta*, 990, 87–92.
- Hasan, S.S., Stofleth, J.T., Yamashita, E. & Cramer, W.A. (2013) Lipid-induced conformational changes within the cytochrome *b₆f* complex of oxygenic photosynthesis. *Biochemistry*, 52, 2649–2654.
- Horsch, R.B., Fry, J.E., Hoffmann, N.L., Wallroth, M., Eichholtz, D., Rogers, S.G. et al. (1985) A simple and general method for transferring genes into plants. *Science*, 227, 1229–1231.
- Johnson, J.E. & Berry, J.A. (2021) The role of cytochrome *b₆f* in the control of steady-state photosynthesis: a conceptual and quantitative model. *Photosynthesis Research*, 148, 101–136.
- Johnson, M.P., Pérez-Bueno, M.L., Zia, A., Horton, P. & Ruban, A.V. (2009) The zeaxanthin-independent and zeaxanthin-dependent *qE* components of nonphotochemical quenching involve common conformational changes within the photosystem II antenna in *Arabidopsis*. *Plant Physiology*, 149, 1061–1075.
- Kanazawa, A. & Kramer, D.M. (2002) In vivo modulation of nonphotochemical exciton quenching (NPQ) by regulation of the chloroplast ATP synthase. *Proceedings of the National Academy of Sciences of the United States of America*, 99, 12789–12794.
- Keller, B., Matsubara, S., Rascher, U., Pieruschka, R., Steier, A., Kraska, T. et al. (2019) Genotype specific photosynthesis × environment interactions captured by automated fluorescence canopy scans over two fluctuating growing seasons. *Frontiers in Plant Science*, 10, 1482.

- Keller, B., Vass, I., Matsubara, S., Paul, K., Jedmowski, C., Pieruschka, R. et al. (2019) Maximum fluorescence and electron transport kinetics determined by light-induced fluorescence transients (LIFT) for photosynthesis phenotyping. *Photosynthesis Research*, 140, 221–233.
- Kolber, Z.S., Prášil, O. & Falkowski, P.G. (1998) Measurements of variable chlorophyll fluorescence using fast repetition rate techniques: defining methodology and experimental protocols. *Biochimica et Biophysica Acta (BBA)*. *Bioenergetics*, 1367, 88–106.
- Kramer, D.M. & Crofts, A.R. (1989) Activation of the chloroplast ATPase measured by the electrochromic change in leaves of intact plants. *Biochimica et Biophysica Acta (BBA)* - *Bioenergetics*, 976, 28–41.
- Kromdijk, J., Głowacka, K., Leonelli, L., Gabilly, S.T., Iwai, M., Niyogi, K.K. et al. (2016) Improving photosynthesis and crop productivity by accelerating recovery from photoprotection. *Science*, 354, 857–861.
- Kügler, M., Jänsch, L., Kruff, V., Schmitz, U.K. & Braun, H.-P. (1997) Analysis of the chloroplast protein complexes by blue-native polyacrylamide gel electrophoresis (BN-PAGE). *Photosynthesis Research*, 53, 35–44.
- Lefebvre, S., Lawson, T., Fryer, M., Zakhleniuk, O.V., Lloyd, J.C. & Raines, C.A. (2005) Increased sedoheptulose-1,7-bisphosphatase activity in transgenic tobacco plants stimulates photosynthesis and growth from an early stage in development. *Plant Physiology*, 138, 451–460.
- Long, S.P., Zhu, X.G., Naidu, S.L. & Ort, D.R. (2006) Can improvement in photosynthesis increase crop yields? *Plant Cell and Environment*, 29, 315–330.
- López-Calcano, P.E., Brown, K.L., Simkin, A.J., Fisk, S.J., Violet-Chabrand, S., Lawson, T. et al. (2020) Stimulating photosynthetic processes increases productivity and water-use efficiency in the field. *Nature Plants*, 6, 1054–1063.
- López-Calcano, P.E., Fisk, S., Brown, K.L., Bull, S.E., South, P.F. & Raines, C.A. (2019) Overexpressing the H-protein of the glycine cleavage system increases biomass yield in glasshouse and field-grown transgenic tobacco plants. *Plant Biotechnology Journal*, 17, 141–151.
- Malone, L.A., Proctor, M.S., Hitchcock, A., Hunter, C.N. & Johnson, M.P. (2021) Cytochrome b6f—Orchestrator of photosynthetic electron transfer. *Biochimica et Biophysica Acta (BBA)* - *Bioenergetics*, 1862, 148380.
- Martin-Avila, E., Lim, Y.-L., Birch, R., Dirk, L.M.A., Buck, S., Rhodes, T. et al. (2020) Modifying plant photosynthesis and growth via simultaneous chloroplast transformation of rubisco large and small subunits. *The Plant Cell*, 32, 2898–2916.
- Molik, S., Karnauchov, I., Weidlich, C., Herrmann, R.G. & Klösgen, R.B. (2001) The Rieske Fe/S protein of the cytochrome b₆f complex in chloroplasts: MISSING LINK IN THE EVOLUTION OF PROTEIN TRANSPORT PATHWAYS IN CHLOROPLASTS? *Journal of Biological Chemistry*, 276, 42761–42766.
- Mould, R.M., Kapazoglou, A. & Gray, J.C. (2001) Assembly of cytochrome f into the cytochrome b₆f complex in isolated pea chloroplasts. *European Journal of Biochemistry*, 268, 792–799.
- Ort, D.R., Merchant, S.S., Alric, J., Barkan, A., Blankenship, R.E., Bock, R. et al. (2015) Redesigning photosynthesis to sustainably meet global food and bioenergy demand. *Proceedings of the National Academy of Sciences of the United States of America*, 112, 8529–8536.
- Osmond, B., Chow, W.S., Pogson, B.J. & Robinson, S.A. (2019) Probing functional and optical cross-sections of PSII in leaves during state transitions using fast repetition rate light induced fluorescence transients. *Functional Plant Biology*, 46, 567–583.
- Osmond, C.B., Chow, W.S. & Robinson, S.A. (2022) Inhibition of non-photochemical quenching increases functional absorption cross-section of photosystem II as excitation from closed reaction centres is transferred to open centres, facilitating earlier light saturation of photosynthetic electron transport. *Functional Plant Biology*, 49, 463–482.
- Parry, M.A.J., Andralojc, P.J., Scales, J.C., Salvucci, M.E., Carmo-Silva, A.E., Alonso, H. et al. (2013) Rubisco activity and regulation as targets for crop improvement. *Journal of Experimental Botany*, 64, 717–730.
- Porra, R.J., Thompson, W.A. & Kriedemann, P.E. (1989) Determination of accurate extinction coefficients and simultaneous equations for assaying chlorophylls a and b extracted with four different solvents: verification of the concentration of chlorophyll standards by atomic absorption spectroscopy. *Biochimica et Biophysica Acta (BBA)* - *Bioenergetics*, 975, 384–394.
- Price, G.D., von Caemmerer, S., Evans, J.R., Siebke, K., Anderson, J.M. & Badger, M.R. (1998) Photosynthesis is strongly reduced by antisense suppression of chloroplastic cytochrome b₆f complex in transgenic tobacco. *Australian Journal of Plant Physiology*, 25, 445–452.
- Price, G.D., Yu, J.-W., von Caemmerer, S., Evans, J.R., Chow, W.S., Anderson, J.M. et al. (1995) Chloroplast cytochrome b₆/f and ATP synthase complexes in tobacco: transformation with antisense RNA against nuclear-encoded transcripts for the Rieske FeS and ATP δ polypeptides. *Australian Journal of Plant Physiology*, 22, 285–297.
- Ray, D.K., Mueller, N.D., West, P.C. & Foley, J.A. (2013) Yield trends are insufficient to double global crop production by 2050. *PLoS One*, 8, e66428.
- Ruban, A.V. (2016) Nonphotochemical chlorophyll fluorescence quenching: mechanism and effectiveness in protecting plants from photodamage. *Plant Physiology*, 170, 1903–1916.
- Ruuska, S.A., Andrews, T.J., Badger, M.R., Price, G.D. & von Caemmerer, S. (2000) The role of chloroplast electron transport and metabolites in modulating rubisco activity in tobacco. Insights from transgenic plants with reduced amounts of cytochrome b₆/f complex or glyceraldehyde 3-phosphate dehydrogenase. *Plant Physiology*, 122, 491–504.
- Schmidt, G.W. & Delaney, S.K. (2010) Stable internal reference genes for normalization of real-time RT-PCR in tobacco (*Nicotiana tabacum*) during development and abiotic stress. *Molecular Genetics and Genomics*, 283, 233–241.
- Schöttler, M.A., Tóth, S.Z., Boulouis, A. & Kahlau, S. (2015) Photosynthetic complex stoichiometry dynamics in higher plants: biogenesis, function, and turnover of ATP synthase and the cytochrome b₆f complex. *Journal of Experimental Botany*, 66, 2373–2400.
- Sharkey, T.D., Bernacchi, C.J., Farquhar, G.D. & Singsaas, E.L. (2007) Fitting photosynthetic carbon dioxide response curves for C₃ leaves. *Plant Cell and Environment*, 30, 1035–1040.
- Simkin, A.J., McAusland, L., Lawson, T. & Raines, C.A. (2017) Overexpression of the RieskeFeS protein increases electron transport rates and biomass yield. *Plant Physiology*, 175, 134–145.
- Tikhonov, A.N. (2014) The cytochrome b₆f complex at the crossroad of photosynthetic electron transport pathways. *Plant Physiology and Biochemistry*, 81, 163–183.
- von Caemmerer, S. & Farquhar, G.D. (1981) Some relationships between the biochemistry of photosynthesis and the gas exchange of leaves. *Planta*, 153, 376–387.
- Walter, J. & Kromdijk, J. (2022) Here comes the sun: how optimization of photosynthetic light reactions can boost crop yields. *Journal of Integrative Plant Biology*, 64, 564–591.
- Wilson, S., Johnson, M.P. & Ruban, A.V. (2021) Proton motive force in plant photosynthesis dominated by Δ pH in both low and high light. *Plant Physiology*, 187, 263–275.
- Yamori, W., Evans, J.R. & von Caemmerer, S. (2010) Effects of growth and measurement light intensities on temperature dependence of CO₂ assimilation rate in tobacco leaves. *Plant Cell and Environment*, 33, 332–343.
- Yamori, W., Kondo, E., Sugiura, D., Terashima, I., Suzuki, Y. & Makino, A. (2016) Enhanced leaf photosynthesis as a target to increase grain yield: insights from transgenic rice lines with variable Rieske FeS protein content in the cytochrome b₆/f complex. *Plant Cell and Environment*, 39, 80–87.

Yamori, W., Takahashi, S., Makino, A., Price, G.D., Badger, M.R. & von Caemmerer, S. (2011) The roles of ATP synthase and the cytochrome *b(6)/f* complexes in limiting chloroplast electron transport and determining photosynthetic capacity. *Plant Physiology*, 155, 956–962.

SUPPORTING INFORMATION

Additional supporting information can be found online in the Supporting Information section at the end of this article.

How to cite this article: Heyno, E., Ermakova, M., Lopez-Calcagno, P.E., Woodford, R., Brown, K.L., Matthews, J. S.A. et al. (2022) Rieske FeS overexpression in tobacco provides increased abundance and activity of cytochrome *b₆f*. *Physiologia Plantarum*, 174(6), e13803. Available from: <https://doi.org/10.1111/ppl.13803>